M&C 2017 - International Conference on Mathematics & Computational Methods Applied to Nuclear Science & Engineering, Jeju, Korea, April 16-20, 2017, on USB (2017)

Subplane-based Control Rod Decusping Techniques for the 2D/1D Method in MPACT[1]

Aaron M. Graham,* Benjamin S. Collins,† Thomas Downar*

*Department of Nuclear Engineering and Radiological Sciences, University of Michigan, Ann Arbor, MI
†Reactor Physics Group, Oak Ridge National Laboratory, P.O. Box 2008, Oak Ridge, TN
aarograh@umich.edu, collinsbs@ornl.gov, downar@umich.edu

Abstract - *The MPACT transport code is being jointly developed by Oak Ridge National Laboratory and the University of Michigan to serve as the primary neutron transport code for the Virtual Environment for Reactor Applications Core Simulator. MPACT uses the 2D/1D method to solve the transport equation by decomposing the reactor model into a stack of 2D planes. A fine mesh flux distribution is calculated in each 2D plane using the method of characteristics (MOC), and then the planes are coupled axially by using the 1D P_3 approximation wrapped in a two-node nodal expansion method (NEM-P_3) solver. This iterative calculation is then accelerated using the coarse mesh finite difference method (CMFD).*

Control rod cusping is a problem that arises frequently when using the 2D/1D method. This occurs when the tip of a control rod falls between the boundaries of an MOC plane, requiring that the rodded and unrodded regions be axially homogenized for the 2D MOC calculations. Performing a volume homogenization does not properly preserve the reaction rates due to an error known as cusping. The most straightforward way to resolve this problem is by refining the axial mesh, but this can significantly increase the computational expense of the calculation. The other way of resolving the partially inserted rod is through the use of a decusping method. This paper presents new decusping methods implemented in MPACT that can dynamically correct the rod cusping behavior for a variety of problems.

I. INTRODUCTION

The Consortium for Advanced Simulation of Light-Water Reactors (CASL) [1] is developing an advanced code package called the Virtual Environment for Reactor Applications (VERA). VERA is intended to provide tools for high-fidelity modeling and simulation of LWRs beyond what has been historically been possible with tools available to industry. These tools include codes to perform neutronics, thermal-hydraulics, fuel performance, and other calculations, as shown in Figure 1. MPACT is the deterministic neutronics code in VERA and uses the 2D/1D method to provide 3D pin-resolved power distributions for the entire reactor [2, 3]. The work discussed in this paper focuses on improvements made to control rod decusping techniques in MPACT's 2D/1D implementation using the subplane scheme.

The 2D/1D method [3, 4, 5, 6] takes advantage of the geometry in the reactor by noting that most heterogeneity occurs in the radial direction. Therefore, the problem is decomposed into a stack of 2D planes. In MPACT, each radial plane is solved using the 2D method of characteristics (MOC), which is capable of resolving complicated geometries accurately. These planes are then coupled in the axial direction using the 1D P_3 approximation wrapped in a two-node Nodal Expansion Method (NEM-P_3) solver [7, 8] that performs calculations on a coarse, pin-homogenized mesh. Additionally, this scheme uses 3D coarse mesh finite difference (CMFD) [9] to accelerate the convergence of the solution. This iteration scheme can provide highly accurate 3D power distributions, and it is still much faster than performing a direct 3D transport calculation.

One significant requirement for the 2D/1D method to provide accurate results is that the materials be axially homogeneous in each 2D MOC plane. Typically, this is accomplished by correctly meshing the problem so that MOC plane boundaries align with axial heterogeneities. However, for long calculations with moving control rods, selecting an axial mesh to resolve all the control rod positions can be tedious and may dramatically increase computational requirements.

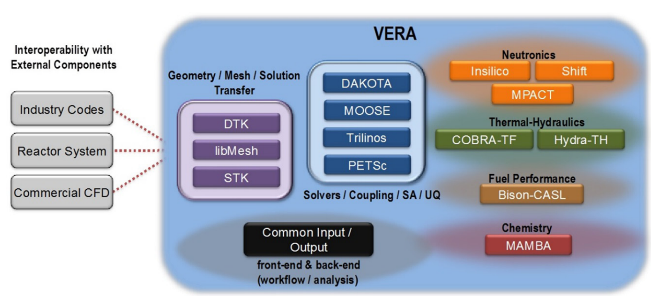

Fig. 1. VERA code package.

[1]This manuscript has been authored by UT-Battelle, LLC, under Contract No. DE-AC0500OR22725 with the U.S. Department of Energy. The United States Government retains and the publisher, by accepting the article for publication, acknowledges that the United States Government retains a nonexclusive, paid-up, irrevocable, worldwide license to publish or reproduce the published form of this manuscript, or allow others to do so, for the United States Government purposes. The Department of Energy will provide public access to these results of federally sponsored research in accordance with the DOE Public Access Plan (http://energy.gov/downloads/doe-public-access-plan).

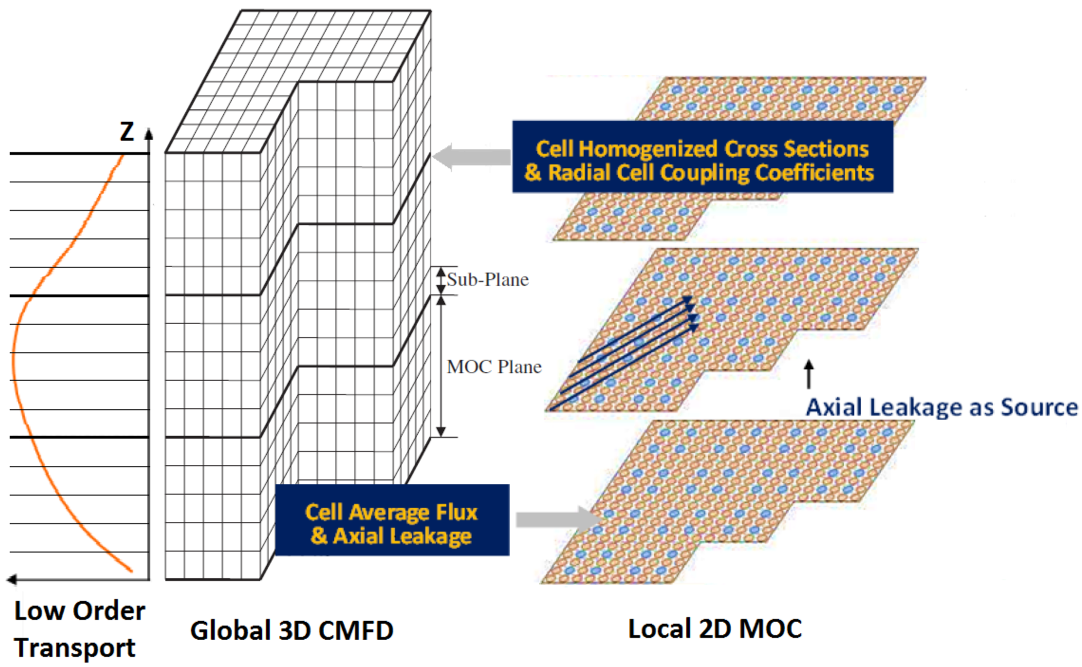

Fig. 2. 2D/1D method with the subplane scheme used for the 3D CMFD and 1D axial calculations.

Thus, other methods are required to address the problem of a partially inserted control rod.

II. THEORY

The problem of rod cusping is described below, followed by a brief description of the subplane CMFD and NEM-P_3 calculations. Lastly, each of the three decusping techniques implemented in MPACT are described.

1. Rod Cusping

The rod cusping effect occurs when a strong absorber such as a control rod is partially inserted into an MOC plane. Because the MOC calculations are 2D in the radial direction, the control rod must be homogenized with the material underneath it. This is normally done up front with a simple volume homogenization to preserve the volume and mass of the control rod. However, because the strong absorber is smeared downward across the entire plane, this introduces an artificial dip in the local flux and global reactivity, as shown in Figure 3 [10].

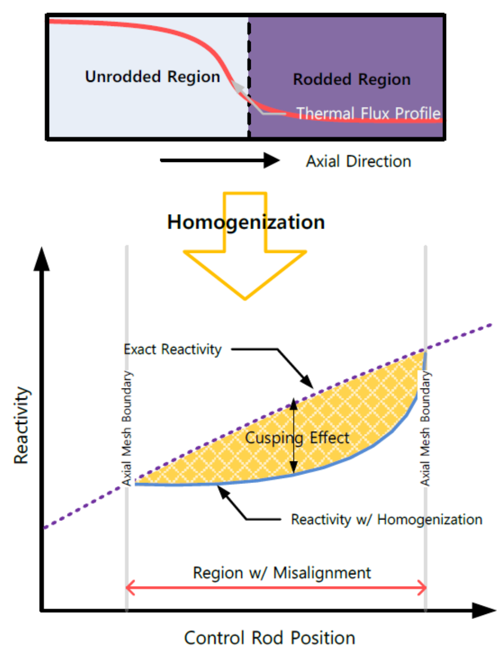

Fig. 3. Control rod cusping effects [10].

2. Subplane CMFD and NEM-P_3

The CMFD method is used to accelerate the convergence of transport calculations. The fine mesh used by the MOC calculations usually has approximately 50 regions per pin cell. To accelerate the convergence, each pin cell is homogenized into a single region, preserving total reaction rates in the pin cell. A 3D diffusion calculation is then performed to obtain a global flux shape. After this calculation is complete, the CMFD flux shape is projected back to the MOC mesh to scale the magnitude of the fine mesh flux solution and to accelerate it.

Because CMFD uses the diffusion approximation, the currents in the axial direction used to couple the MOC planes will not be accurate. To prevent this, a 1D NEM-P_3 calculation is performed on the homogenized coarse mesh. This calculation uses NEM to capture the spatial shape of the flux and the 1D P_3 method to capture the angular shape of the flux, resulting in more accurate interface currents to couple the MOC planes. In MPACT, this calculation is performed after the 3D CMFD solve and before the 2D MOC solve.

Refining the axial mesh in 2D/1D by using a large number of thin MOC planes will improve the accuracy of the calculations. However, because the MOC planes are the most expensive part of 2D/1D, refining the mesh can significantly increase runtime. Furthermore, thin MOC planes require more under-relaxation for the 2D/1D iteration scheme to remain stable [11], further increasing the runtime. Because of this, a balance must be struck in the axial mesh to obtain sufficiently accurate solutions without excessively burdensome computational cost, limiting the mesh refinement that can be done to prevent rod cusping.

To do obtain this balance, the subplane scheme [12] was implemented in MPACT [13]. This method divides each MOC plane into multiple subplanes for the CMFD and 1D axial calculations while still using just one plane for the MOC calculations. This ensures that the CMFD cells remain sufficiently thin to prevent instabilities, and it increases the accuracy of the CMFD and NEM-P_3 calculations without increasing the computational burden from the MOC calculations.

3. Decusping Methods

One downside to decreasing the number of MOC planes is that partially inserted control rods, and thus rod cusping effects, become more important. To alleviate this, new control rod decusping methods are being developed to work in conjunction with the subplane method. This section describes three different decusping methods available in MPACT. The first is the default method that was already available in MPACT and does not use the subplane scheme at all. The other two are new methods that make use of the subplane scheme to provide more general, accurate decusping capabilities.

A. Polynomial Decusping

The polynomial decusping uses pregenerated functions to adjust the volume fraction of the control rod during the homogenization step [14]. To generate these functions, two series of simulations were completed on 3×3 assembly cases with a rod inserted in the center assembly. The first series of cases had the rod at various partially inserted positions in an MOC plane. The second series repeated these calculations with extra MOC planes to eliminate the need for homogenization. The k_{eff} values for each of these cases was then used to generate a sixth-order polynomial of the reactivity as a function of rod insertion into a plane. The partially inserted control rod volume fraction is then reduced according to the expected reactivity error modeled by the polynomial. This procedure was done for AIC, B_4C, and Tungsten control rod materials, allowing it to be useful for most pressurized water reactor (PWR) models of interest.

B. Subplane Decusping

The subplane scheme traditionally uses the same cross-sections for all subplane cells in an MOC pin cell. However, this does nothing to address a partially inserted rod. To improve the subplane scheme to capture axial heterogeneities, modifications were made to both the subplane and MOC cross-sections. When performing the cross-section homogenization for CMFD, regions where the control rod was homogenized use unrodded cross-sections in the lower subplanes and rodded cross-sections in the upper subplanes, as opposed to using a single homogenized cross-section in all subplanes. This modification allows the CMFD calculations to capture the sharp gradient in the axial flux profile around the rod tip instead of a more gradual change in the flux due to homogenized cross-sections.

After the CMFD calculation and projection to the MOC mesh, the MOC cross-sections are then modified to account for the axial flux shape from the subplane CMFD calculations. To do this, the subplane fluxes are used with the rodded and unrodded cross-sections to perform a flux-volume homogenization as opposed to performing volume homogenization or using the polynomial decusping method as might normally be done. This calculation is shown in Equation 1:

$$\overline{\Sigma_i} = \frac{\sum_{j\in J} \phi^j_{rad,i}\phi^j_{ax,i}\Sigma^j_i h^j}{\sum_{j\in J} \phi^j_{rad,i}\phi^j_{ax,i} h^j} \tag{1}$$

where superscript j denotes the axial level, J indicates the total number of axial levels in each MOC plane, i is the radial cross-section region index on the MOC mesh, ϕ_{ax} is the cell-averaged sub-plane flux, ϕ_{rad} is the average flux in cross-section region i, Σ_i is the cross-section in region i, h is the height of the axial level, and $\overline{\Sigma_i}$ is the homogenized cross-section used by the MOC calculations. In addition to capturing the effects of a partially inserted rod, this expression can also capture cases in which a heterogeneous rod might cause cusping effects at material interfaces within the rod. For subplane decusping, $\phi^j_{rad,i}$ is the same for all axial levels. This will not be true in the following section in which both axial and radial effects of the rod are captured.

C. Collision Probabilities Decusping

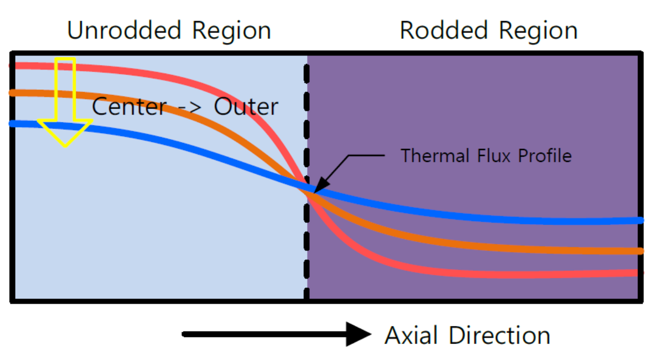

Fig. 4. Radial variation in axial flux profiles for a partially rodded pin cell [10].

The subplane decusping scheme described above captures the axial effects of the partially inserted rod. However, the radial flux shapes used to calculate the subplane CMFD cross-sections are those generated by the 2D MOC calculations. These calculations were performed using homogenized cross-sections and do not accurately reflect the radial shape in either the rodded or unrodded regions. Figure 4 [10] shows axial flux profiles in a partially rodded node as a function of radial position, an effect that cannot be captured using homogenized cross-sections in MOC. To account for these effects, the collision probabilities (CP) method [15] can be applied. In this method, the partially rodded pin cell is cylindricized by changing the moderator region to an annulus while preserving the volume. Then the surrounding pin cells are flux-volume homogenized into an additional ring outside the moderator. This buffer region is added to provide a fission source to drive the CP calculations. With the moderator and buffer regions set up, 1D CP calculations can be carried out, first with the rodded cross-sections, then with the unrodded cross-sections.

These calculations give a unique radial flux profile for each axial region of the partially inserted rod. These radial profiles are then used in place of the MOC flux when performing the cross-section homogenization described in the previous section. This further improves the accuracy of the subplane CMFD calculations for the partially inserted rod by allowing the CMFD cross-sections to capture some of the radial effects of the rod, as well as the axial effects. After the CMFD calculations are completed, the MOC cross-sections are then homogenized using Equation 1, as with the subplane decusping. An illustration of the CP calculations is shown in Figure 5.

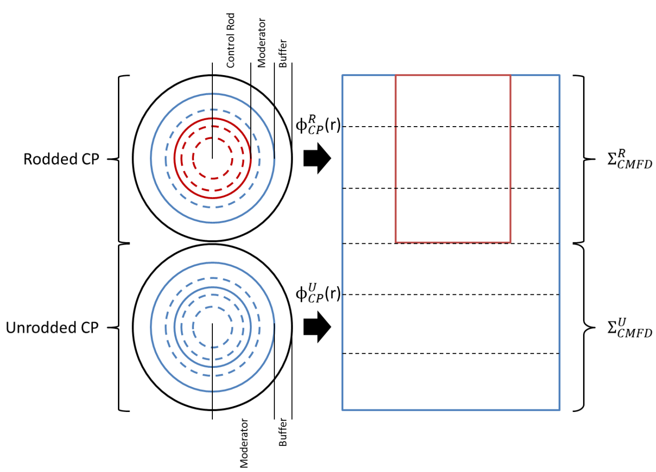

Fig. 5. Decusping with subplane scheme and 1D collision probabilities.

III. RESULTS AND ANALYSIS

To test the effectiveness of each of these decusping methods, Problem 4 from the VERA Progression Problems [16] was selected. This is a 3×3 assembly problem with a control rod in the center assembly. The assemblies are Westinghouse 17×17 assemblies with an active fuel height of 365.76 cm. Each assembly has 6 spacer grids 3.810 cm in height in the active fuel region. Using conventional 2D/1D in MPACT, this problem would normally be simulated using a total of 58 MOC planes and 49 planes in the active fuel region. Each spacer grid is 1 plane, and the spans between grids are divided into 6 planes of about 8 cm each. An example fuel assembly is shown in Figure 6, and the radial layout of Problem 4 is shown in Figure 7.

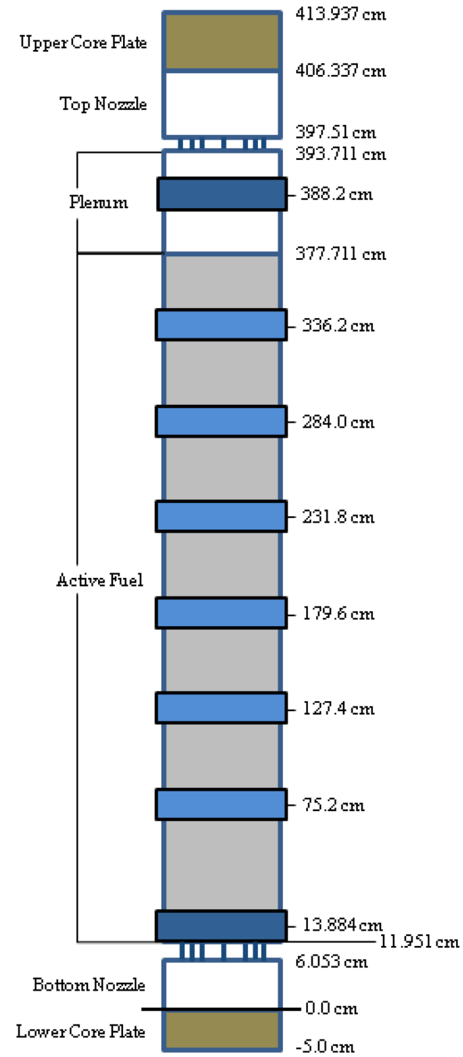

Fig. 6. Axial description of Westinghouse 17×17 fuel assembly in Watts Bar Unit 1.

2.1	2.6 20 PY	2.1
2.6 20 PY	2.1 RCCA	2.6 20 PY
2.1	2.6 20 PY	2.1

Fig. 7. VERA Problem 4 assembly layout.

The control rod described in this model is a heterogeneous rod. It consists of an AIC poison with a B_4C follower and stainless steel tip. This heterogeneous design introduces

TABLE I. Comparison of Rod Decusping Methods in MPACT for VERA Progression Problem 4 for Homogeneous Control Rods

Rod Material	Case	k_{eff} Difference (pcm)	Pin Power Differences RMS	Max	2D/1D Iterations	Runtime (Core-Hours)
AIC	Reference	–	–	–	15	19.6
	No treatment	−29.5	1.531%	11.839%	12	14.7
	Polynomial	−0.3	0.444%	4.081%	12	14.3
	Subplane	−11.5	0.726%	8.209%	12	14.2
	Subplane + 1D-CP	−5.6	0.368%	4.248%	12	15.3
B_4C	Reference	–	–	–	15	16.9
	No treatment	112.0	6.978%	69.372%	12	12.7
	Polynomial	112.6	6.886%	66.731%	12	12.1
	Subplane	−17.9	1.142%	11.357%	13	15.2
	Subplane + 1D-CP	−11.0	0.687%	6.367%	12	13.4
Tungsten	Reference	–	–	–	15	23.5
	No treatment	−8.4	0.370%	3.374%	12	15.5
	Polynomial	−4.4	0.239%	2.720%	12	14.5
	Subplane	1.6	0.069%	0.598%	12	13.9
	Subplane + 1D-CP	−0.9	0.055%	0.941%	12	15.6

cusping-like effects at each material interface in the rod rather than just at the tip, making this model useful for testing the decusping methods for a variety of material combinations. This section will discuss results for three different groups of simulations based on VERA Problem 4: homogeneous control rod, heterogeneous control rod, and rod worth calculations.

1. Homogeneous Control Rod

To isolate the effects of cusping and the accuracy of the decusping methods, VERA Problem 4 was modified, replacing the heterogeneous control rod with a homogeneous control rod made of either AIC, B_4C, or tungsten. The rods were withdrawn 88 steps to position the tip at an elevation of 155.9875 cm, about 144 cm above the bottom of the active fuel. This position caused the tip of the rod to be partially inserted into an MOC plane extending from 153.5 cm to 165.5975 cm, causing severe rod cusping.

These calculations were run on a small development cluster with 2.3 GHz AMD processors (Opteron^{TM} Processor 6376). Each of the decusping cases used 43 MOC planes, corresponding to one plane per spacer grid with 4 planes between each pair of grids. Each MOC plane was divided into enough subplanes so that each subplane was no more than 8 cm thick. The reference case used the same meshing parameters with an extra MOC plane boundary aligned with the tip of the control rod. This ensured no cusping effects were present in the reference case.

The results of the homogeneous rod calculations are shown in Table I. The B_4C rod uses the strong thermal absorber boron, causing it to have the largest errors. Furthermore, this prevents the polynomial decusping from being effective in resolving the partially inserted rod. The subplane decusping greatly improves the result, indicating that for this rod, the axial effects are dominant. However, obtaining a more accurate radial shape from the CP calculations significantly improves on the subplane result. The errors while using subplane and CP are still higher than desired for 2D/1D calculations but are more acceptable than with no treatment or the polynomial decusping method.

The AIC rod causes much smaller errors than the B_4C rod. For this rod, the polynomial decusping performs reasonably well, with a maximum pin power error of about 4%. The errors in the subplane decusping method without 1D CP are much larger than in the polynomial decusping. The AIC rod is strongly absorbing at higher energies than the B_4C rod, and silver, indium, and cadmium all have resonances in their absorption cross-sections. Because of this, the lack of a radial correction in the subplane decusping produces unacceptably large errors. Finally, when using the 1D CP calculations as well, the errors are much smaller than without. The maximum power difference is slightly larger than for the polynomial decusping, but the k_{eff} difference is negligibly small and the RMS power difference is better.

Because the tungsten rod is a gray rod, the cusping errors it produces are much smaller than for the other two rods. The polynomial decusping still reduces the errors, but by much less than for the AIC rod. Both subplane-based methods reduce the maximum power distribution error to less than 1%, with the 1D CP producing a higher maximum error but lower RMS error. Overall, all three methods perform well on this rod, and the subplane-based methods reduce the errors to levels that may be acceptable for certain applications of the 2D/1D method in MPACT.

Table I also shows the number of iterations and core-hours required for each calculation. In the reference case, the extra MOC plane boundary causes a 2.5 cm thick MOC plane to be present. This forces the 2D/1D iteration to use more under-relaxation to remain stable, slowing the convergence of the problem. Since the cases using the decusping methods do

TABLE II. Comparison of Rod Decusping Methods in MPACT for VERA Progression Problem 4 for Heterogeneous Control Rod

Case	k_{eff} Difference (pcm)	Pin Power Differences RMS	Max	2D/1D Iterations	Runtime (Core-Hours)
Reference	–	–	–	15	16.6
No treatment	−45.9	2.427%	20.450%	12	13.8
Polynomial	−2.5	0.457%	5.067%	12	13.0
Subplane	−17.3	1.101%	11.771%	13	14.9
Subplane + 1D-CP	−5.5	0.415%	3.866%	12	14.7

not have this thin plane, they converge in 12 iterations (except for one case which required 13) instead of 15 iterations. This reduction in iterations reduces the runtime of the calculations using the decusping methods. The decusping cases also used slightly fewer cores than the reference cases, further contributing to the reduction in core-hours observed by each of the decusping methods.

In general, the subplane-based decusping techniques are slightly slower than the polynomial decusping method. The 1D CP calculations are efficient enough that they are negligible compared to the total calculation time, and the 2D MOC and 1D NEM-P_3 calculations perform a fixed number of inner iterations for each 2D/1D outer iteration. This indicates that the additional runtime incurred by the subplane-based methods is due to the CMFD calculations. This occurs because the changes to the cross-sections used by CMFD affects the convergence of the linear solver. Thus, the subplane-based methods require a few more CMFD inner iterations during the first few 2D/1D outer iterations, causing a small increase in the total runtime.

2. Heterogeneous Control Rod

The homogeneous rod calculations were repeated using the full heterogeneous rod from the original VERA Problem 4 specifications. This rod has three interfaces of interest: the tip of the stainless steel plug in contact with moderator, the interface between the plug and the AIC absorber, and the interface between the AIC and the B_4C follower. The rod was withdrawn to 88 steps, so these interfaces were located at positions of 155.9875, 157.8875, and 259.4875. The first two interfaces fell within the same MOC plane extending from 153.5 cm to 165.5975 cm, and the third interface was in a different MOC plane extending from 257.9 cm to 269.9975 cm.

Again, each of the decusping cases again 43 MOC planes for the heterogeneous rod. The reference case had 3 extra MOC plane boundaries added to eliminate cusping effects at each of the 3 control rod interfaces, resulting in a total of 46 MOC planes for the reference case. All 5 cases were run using 1 core per plane.

Table II shows results for the heterogeneous rod calculations. Again it can be seen that using subplane with 1D-CP performs most effectively. The k_{eff} result is slightly less accurate than with the polynomial decusping since the polynomials were generated based on k_{eff}. However, the power comparisons are more accurate with the 1D-CP method, reducing the maximum pin power error to 3.117%. The subplane decusping without the 1D-CP corrections performs the least accurately of the three methods, with a maximum power difference of 10.668%. This shows the importance of capturing the radial self-shielding effects in the rodded region of the MOC plane. Ignoring these effects overestimates the absorption and introduces significant errors.

It should also be noted that the 1D-CP decusping is capturing the effects of the stainless steel rod plug, while the polynomial decusping ignores the stainless steel completely. While effect of the steel is small compared to the other materials in the rod, it is contributing to the effects some. The 1D-CP decusping can capture these effects on the fly, while the polynomial decusping cannot currently account for them. The subplane decusping without 1D-CP treats the axial effects of the stainless steel, but not the radial effects.

As with the homogeneous rods, a significant improvement in runtime is observed for the decusping methods compared to the refined mesh reference case. Calculations with the decusping methods converged in 12 iterations instead of 15 due to thicker MOC planes. Furthermore, 3 fewer cores were required for the calculations, further contributing to the decrease in core-hours required for the calculations.

3. Rod Worth Calculations

The last set of calculations used to test MPACT's decusping methods is a set of rod worth calculations. For these calculations, VERA Problem 4 was simulated with the heterogeneous rod at every position from 0 steps to 230 steps withdrawn. The differential rod worth was then defined as total change in k_{eff} in pcm divided by the number of steps withdrawn. This was done using each of the three decusping methods and once with no decusping treatment. This shows the effects of rod cusping and the decusping techniques as the rod moves through various planes in the model.

Because of the number of calculations required, the mesh was coarsened to only 30 MOC planes for all rod worth calculations. The maximum subplane thickness was set to 3.2 cm to maximize accuracy and stability while using the coarse MOC mesh. Each calculation was performed using 270 cores on Titan [17], so each quarter assembly in each plane was on a single core.

The differential rod worth curves are shown in Figure 8. The blue markers show the cusping effects of the rod when

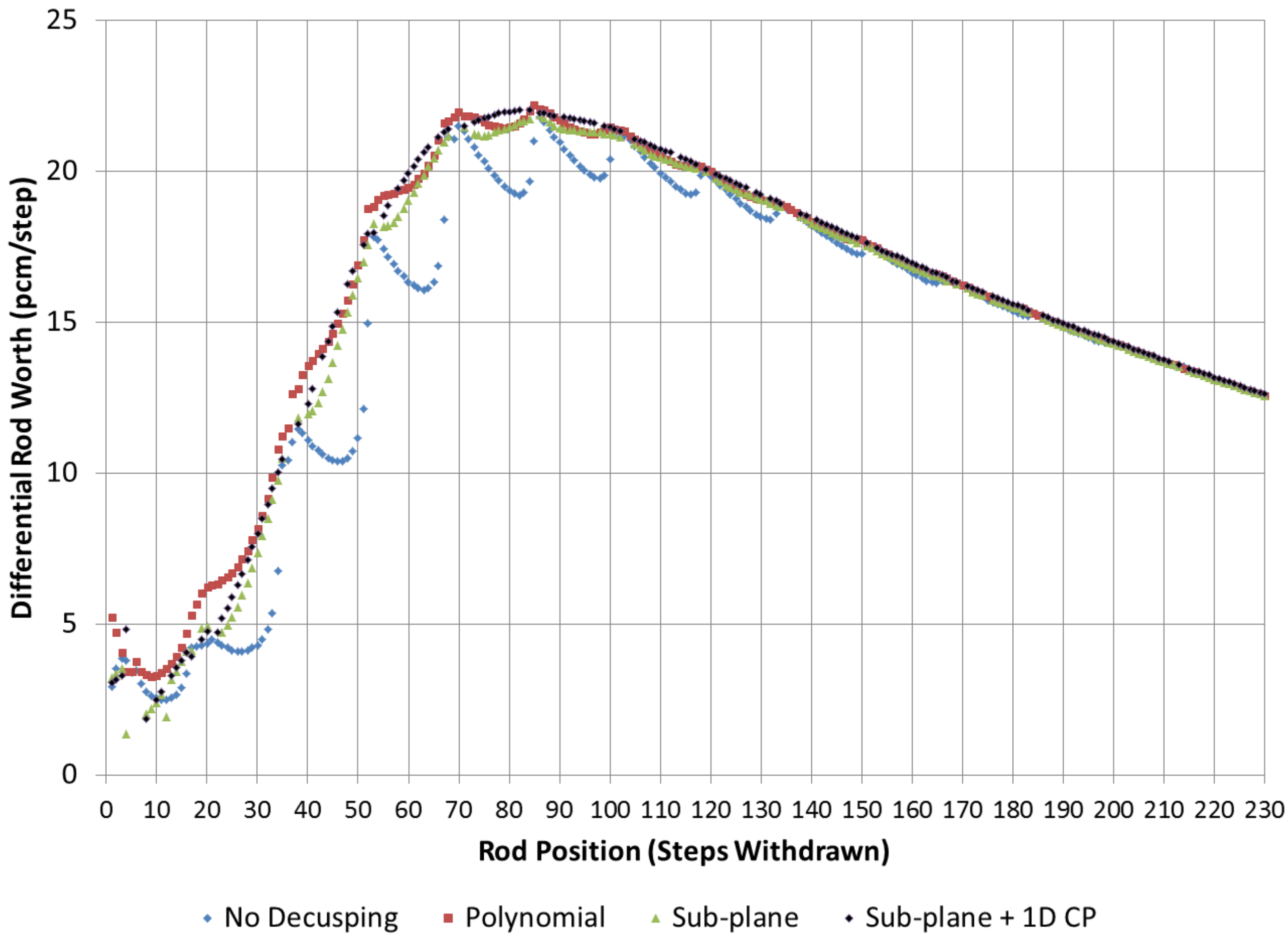

Fig. 8. Differential rod worth curves for MPACT decusping techniques.

no decusping treatment is used. The polynomial decusping prevents the large cusps seen with no decusping treatment. However, in the lower half of the core, there are still some large fluctuations from the expected shape. Because the polynomial corrections were generated using a more refined mesh and a single MOC plane, they are susceptible to large errors when the conditions are significantly different from those under which the they were generated. The subplane decusping performs more predictably than the polynomial. It still shows some cusping behavior, but with a much smaller deviation from the expected curve. This occurs because the axial effects are captured reasonably well, but the radial effects are ignored. Finally, the black markers show the subplane decusping with radial 1D-CP. This curve smoothly follows the anticipated shape, showing that this method does the best job capturing the cusping effects.

A problem with the stability is seen in the subplane-based methods as they are currently implemented. At times, a control rod boundary may be very close to an MOC plane boundary. Aligning a subplane with the rod boundary can then result in subplanes less than 1 cm thick. This is sometimes sufficient to prevent the calculations from converging. In Figure 8, the subplane and 1D-CP rod worth curves include a few gaps. These gaps exist because of calculations that diverged due to an extreme axial mesh. Because the polynomial decusping does not rely on subplanes, it does not experience this behavior. However, the implementation of the subplane-based decusping methods can be improved to prevent these types of extreme meshes while still effectively preventing cusping effects.

In addition to looking at the shape of the rod worth curves, the Monte Carlo code KENO-VI [18] was used to develop Monte Carlo reference solutions every 23 steps (10% withdrawal) from 0 to 230 steps. Using these reference solutions, k_{eff} and 3D power distributions can be compared at various points along the differential rod worth curves. The endpoints (0 and 230 steps) were omitted because no significant cusping effects occur in those positions, and the points at 69 and 184 steps are omitted due to convergence difficulties with the subplane-based methods in those configurations.

Table III shows the average k_{eff} and pin power distribution differences for each decusping method for the seven rod positions that had cusping effects and converged solutions for each decusping method. Uncertainties in the Monte Carlo solution have been propagated and are shown for the k_{eff} and

TABLE III. Average Differences between MPACT and KENO-VI for VERA Problem 4

Decusping Method	k_{eff} Difference	Pin Power Difference RMS	Max
None	-24.9 ± 0.6	5.380%	$25.902 \pm 0.097\%$
Polynomial	34.8 ± 0.6	1.502%	$8.957 \pm 0.109\%$
Subplane	34.6 ± 0.6	0.984%	$4.597 \pm 0.094\%$
Subplane + 1D-CP	41.4 ± 0.6	0.763%	$3.386 \pm 0.104\%$

maximum pin power differences. Uncertainties in the RMS are approximately 10^{-5} and therefore not included in the table. The KENO-VI solutions were generated originally for k_{eff} comparisons, so the pin power statistics are not as good as would usually be desired for a Monte Carlo reference solution. However, it is clear from these results that the uncertainties are much smaller than the differences between the decusping solvers, making the comparisons between MPACT and KENO-VI useful.

The subplane decusping with 1D-CP radial treatment is the most accurate on average and for each of the individual positions where comparisons were made, as expected. The average RMS difference is reduced by about half, and the maximum power difference is reduced by nearly a factor of 3. The subplane decusping performed better than the polynomial decusping on average. There were some positions where the polynomial decusping performed comparably to the subplane-based decusping methods, but on average, it was the least effective of the three methods regarding power distributions. For the k_{eff} differences, each of the decusping methods adds about 60 pcm to the uncorrected k_{eff}. The differences between the methods for k_{eff} are insignificant compared to the power distribution results.

IV. CONCLUSIONS AND FUTURE WORK

To address the rod cusping problem in MPACT's 2D/1D method, two new decusping methods were implemented and compared with the old decusping method. It was found that the subplane decusping method with no radial self-shielding treatment was comparable to the old polynomial method, performing better or worse, depending on the problem. However, adding 1D collision probabilities calculations to the subplane decusping consistently showed significant improvements over the other two methods because of the capability to capture the radial effects of the partially inserted rod. It was also shown that using subplane as a foundation for decusping methods prevents the need to refine the axial mesh as much, reducing the runtime and improving the convergence rate in many cases.

While these new methods were shown to be effective, there are several areas of improvement. First, stability is an issue with the subplane-based decusping methods, as seen in the rod worth calculations shown in Figure 8. Because the current implementation requires that subplanes be aligned with the control rod boundaries for the new decusping methods to work properly, CMFD and 1D NEM-P_3 can easily result in very thin cells, which can cause instabilities. This can be addressed in one of two ways. One possible solution is to develop a more stable axial solver that can handle the thin cells. Another solution is modify the decusping solvers so that the subplanes are not required to align exactly with the control rod material boundaries when it might cause instability. The second solution may have some small negative impact on the accuracy of this solution, but it would likely still be much better than the current results from the polynomial decusping.

A second limitation in these decusping solvers is that they are currently unable to account for higher order scattering. The collision probabilities method inherently assumes isotropic scattering, causing the solution to be limited by the accuracy of the transport-corrected cross-sections. Using a different method in lieu of the collision probabilities, such as a small, standalone MOC calculation, would allow higher order scattering to be accounted for.

A third limitation that will be addressed moving forward is the transient problem. The polynomial decusping is currently available for a limited set of transient calculations, but neither of the subplane-based methods support transient calculations yet.

Finally, it is desired to address the cusping problem directly in the 2D MOC calculations if possible. These methods significantly improve the results, but they still rely on cross-section corrections for the MOC portion of the calculation. Moving forward, novel methods for handling the cusping problem directly in the MOC calculation will be combined with the subplane-based methods presented in this paper. Pursuing this type of method should further increase the flexibility and accuracy of the decusping methods in MPACT.

V. ACKNOWLEDGMENTS

This material is based upon work supported under an Integrated University Program Graduate Fellowship.

This research was supported by the Consortium for Advanced Simulation of Light Water Reactors (www.casl.gov), an Energy Innovation Hub (http://www.energy.gov/hubs) for Modeling and Simulation of Nuclear Reactors under U.S. Department of Energy Contract No. DE-AC05-00OR22725.

This research also made use of resources of the Oak Ridge Leadership Computing Facility at the Oak Ridge National Laboratory, which is supported by the Office of Science of the U.S. Department of Energy under Contract No. DE-AC05-00OR22725.

REFERENCES

1. "Consortium for Advanced Simulation of Light Water Reactors (CASL)," Available online. URL www.casl.gov.
2. MPACT TEAM, "MPACT Theory Manual," Tech. rep., Oak Ridge National Laboratory and the University of Michigan (February 2015).
3. B. S. COLLINS, S. STIMPSON, B. W. KELLEY, M. T. H. YOUNG, B. KOCHUNAS, A. GRAHAM, E. W. LARSEN, T. DOWNAR, and A. GODFREY, "Stability and Accuracy of 3D Neutron Transport Simulations Using the 2D/1D Method in MPACT," *Journal of Computational Physics*, **326**, 612–628 (August 2016).
4. J. Y. CHO and H. G. JOO, "Solution of the C5G7MOX Benchmark Three-Dimensional Extension Problems by the DeCART Direct Whole Core Calculation Code," *Prog. Nucl. Energy*, **48**, 456–466 (2006).
5. H. G. JOO, J. Y. CHO, K. S. KIM, C. C. LEE, and S. Q. ZEE, "Methods and Performance of a Three-Dimensional Whole-Core Transport Code DeCART," in "PHYSOR 2004 – The Physics of Fuel Cycles and Advanced Nuclear Systems: Global Developments," Chicago, Illinois (April 25-29 2004).
6. Y. S. JUNG, H. G. JOO, ET AL., "Practical Numerical Reactor Employing Direct Whole Core Neutron Transport and Subchannel Thermal/Hydraulic Solvers," *Ann. Nucl. Energy*, **62**, 357–374 (2013).
7. H. FINNEMANN, F. BENNEWITZ, and M. WAGNER, "Interface current techniques for multidimensional reactor calculations," *Atomkernenergie*, **30**, *2*, 123–128 (1977).
8. R. G. MCCLARREN, "Theoretical Aspects of the Simplified Pn Equations," *Transport Theory and Statistical Physics*, **39**, *2-4*, 73–109 (2011).
9. K. SMITH, "Nodal Method Storage Reduction by Nonlinear Iteration," *Trans. Am. Nucl. Soc.*, **44**, 265 (1983).
10. Y. S. JUNG and H. G. JOO, "Control Rod Decusping Treatment Based on Local 3-D CMFD Calculation for Direct Whole Core Transport Solvers," in "Proceedings of the International Congress on Advances in Nuclear Power Plants (ICAPP)," (April 6–9 2014).
11. B. W. KELLEY, *An Investigation of 2D/1D Approximation to the 3D Boltzmann Transport Equation*, Ph.D. thesis, University of Michigan (2015).
12. J. Y. CHO, K. S. KIM, C. C. LEE, S. Q. ZEE, and H. G. JOO, "Axial SP$_N$ and Radial MOC Coupled Whole Core Transport Calculation," *Journal of Nuclear Science and Technology*, **44**, *9*, 1156–1171 (2007).
13. A. GRAHAM, B. COLLINS, and T. DOWNAR, "Improvement of the 2D/1D Method Using the Sub-Plane Scheme," in "M&C 2017 - International Conference on Mathematics & Computational Methods Applied to Nuclear Science and Engineering," Jeju, Korea (April 16-20 2017).
14. B. M. KOCHUNAS, B. COLLINS, D. JABAAY, S. STIMPSON, A. GRAHAM, K. S. KIM, W. WIESELQUIST, K. CLARNO, S. PALMTAG, T. DOWNAR, and J. GEHIN, "VERA Core Simulator Methodology for PWR Cycle Depletion," in "Proceedings of the ANS Joint International Conference on Mathematics and Computation (M&C 2015), Supercomputing in Nuclear Applications (SNA), and the Monte Carlo (MC) Method," Nashville, TN, USA (April 19–23 2015).
15. D. KNOTT and A. YAMAMOTO, *Handbook of Nuclear Engineering*, D. G. Cacuci (Ed.), chap. Lattice Physics Computations (2010).
16. A. T. GODFREY, "VERA Core Physics Benchmark Progression Problem Specifications," Tech. rep., Oak Ridge National Laboratory (August 2014).
17. "Titan Cray XK7," Available online. URL https://www.olcf.ornl.gov/computing-resources/titan-cray-xk7/.
18. D. F. HOLLENBACH, L. M. PETRIE, and N. F. LANDERS, "KENO-VI: A General Quadratic Version of the KENO Program," in "SCALE: A Modular Code System for Performing Standardized Computer Analysis for Licensing Evaluation, NUREG/CR-0200, Rev. 7 (ORNL/NUREG/CR/CSD-2R7)," Available from the Radiation Safety Information Computational Center at Oak Ridge National Laboratory as CCC-545, vol. II, sect. F17 (April 2004).